The Electronic Spectrum of AuO: A Combined Theoretical and Experimental Study

Leah C. O'Brien,*,† Anne E. Oberlink,† and Björn O. Roos‡

Department of Chemistry, Southern Illinois University, Edwardsville, Illinois 62026-1652, and Department of Theoretical Chemistry, University of Lund, Chemical Center, P.O.B. 124 S-211 00 Lund, Sweden

Received: June 1, 2006; In Final Form: August 30, 2006

The near-infrared electronic spectrum of AuO[1] has been re-examined in light of the new microwave data on the $v = 0$ and $v = 1$ vibrations of the $X^2\Pi_{3/2}$ state of AuO. The two observed bands in the spectrum, with red-degraded bandheads located at 10726 and 10665 cm^{-1}, have been reanalyzed. New theoretical work on AuO clarifies the electronic structure, and the bands in the infrared are now assigned as the (0,1) and (1,2) bands of the $a^4\Sigma^-_{3/2} - X^2\Pi_{3/2}$ transition, respectively.

Introduction

Gas-phase gold oxide, AuO, has been the subject of several recent investigations. In December 2004, the near-infrared spectrum of AuO and the photoelectron spectrum of AuO$^-$ were reported by O'Brien et al.[1] and Ichino et al.,[3] respectively. For the near-infrared spectrum, the two observed bands in the spectrum, with red-degraded bandheads located at 10726 and 10665 cm^{-1}, were assigned as the (0,0) and (1,1) bands of a $^2\Pi_{3/2} - X^2\Pi_{3/2}$ transition, for (v',v''). In January 2005, Okabayashi et al.[2] reported the pure rotational spectrum of AuO in the $X^2\Pi_{3/2}$ state for $v = 0$ and 1. From discrepancies in the ground-state rotational constants between the near-infrared analysis and the microwave analysis, it was clear that the rotational assignments of the near-infrared spectrum were incorrect. In light of the new microwave data, the near-infrared spectrum has been reanalyzed. New theoretical work on the electronic structure of AuO provides insight into the identity of the observed spectrum.

Computational Details

Calculations of the potential curves for AuO were performed using the complete active space self-consistent field (CASSCF) method[4] with dynamic correlation effects added using multiconfigurational perturbation theory (CASPT2).[5,6] Atomic natural orbital basis sets (ANO-RCC) were used, which includes scalar relativistic effects using the Douglas−Kroll−Hess Hamiltonian.[7] Scalar relativistic effects are thus included at all levels of theory. Spin−orbit coupling was added as a last step in the calculation using a recently developed approach where the CASSCF wave functions comprise the basis for a spin−orbit CI calculation with energies shifted to include dynamic correlation.[8] The basis sets used were: Au/8s6p5d3f2g and O/4s3p2d1f. The active space comprised the oxygen 2p,3p and gold 5d,6s orbitals with the corresponding electrons active. The oxygen 3p orbitals were actually not needed and could have been left in the virtual space. The C$_2$ point group was used in order to ensure degeneracy between components of states with $\Lambda \neq 0$.

Calculations were performed on all states that dissociate to ground-state atoms. They are $^4\Sigma^-$, $^2\Sigma^-$, $^4\Pi$, and $^2\Pi$ and give

rise to nine levels with Ω values 5/2, 3/2, 3/2, 3/2, 1/2, 1/2, 1/2, 1/2, and 1/2. A few more states were included in order to ensure that no low-lying levels occurred near equilibrium, which correspond to higher dissociation limits.

Potential curves were generated and spectroscopic constants were obtained by a numerical solution to the rovibrational Schrödinger equation (program VIBROT in MOLCAS). The oscillator strengths were computed by numerical integration of the transition dipole moment functions over appropriate vibrational wave functions for the ground and excited states. Basis set superposition errors were accounted for using the full counter poise method. The size of this error is a good measure of the accuracy of the basis set used. The effect of the correction on the $^2\Pi_{3/2}$ ground state is to lengthen the bond distance 0.007 Å and decrease the bond energy 0.07 eV, yielding results that deviate somewhat more from experiment. We thus conclude that a larger basis set would have given even more accurate results than the ones we present below. All calculations have been performed using the MOLCAS-6 quantum chemistry software.[9]

Theoretical Results

We present the theoretical results in Table 1 for the five lowest levels. An overview of the potentials is presented in Figure 1. The ground state of AuO is $X^2\Pi_{3/2}$. A single bond is formed between the 6s orbital of Au and the 2pσ orbital of O, leaving the oxygen 2pπ orbitals with an electron hole. These orbitals mix with the 5dπ orbitals of AuO, which is the reason for the pronounced spin−orbit splitting between the 3/2 and 1/2 levels of the $X^2\Pi$ state. The spin−orbit splitting is computed to be 1393 cm^{-1}, to be compared to an experimental value of 1440 ± 80 cm^{-1}, obtained from the photoelectron spectroscopy measurement on AuO$^-$.[3] The computed bond distance in our work is $r_e = 1.861$ Å for the $X^2\Pi$ state, which can be compared to an experimental value of $r_e = 1.849$ Å obtained from microwave spectroscopy.[2] A recent CCSD(T) calculation gave $r_e = 1.907$ Å.[3] The same result was obtained using internally contracted MRCI.[3] The improved results obtained here are most likely due to a better description of relativistic effects and a more accurate all-electron basis set. Longer bond distances are obtained using density functional theory (see discussion in ref 3).

The second excited state, the $a^4\Sigma^-_{1/2}$, has a computed T_e value of 11344 cm^{-1}. The next level is the other spin−orbit component

* To whom correspondence should be addressed. Email: lobrien@siue.edu.
† Southern Illinois University.
‡ University of Lund.

Electronic Spectrum of AuO

J. Phys. Chem. A, Vol. 110, No. 43, 2006 **11955**

TABLE 1: Calculated Spectroscopic Parameters for the Lower Electronic States of AuO (Experimental Values within Parentheses)

	$^2\Pi_{3/2}$	$^2\Pi_{1/2}$	$^4\Sigma^-_{1/2}$	$^4\Sigma^-_{3/2}$	$^2\Sigma^+_{1/2}$
R_e (Å)	1.861 (1.849)[a]	1.884	1.921	1.924 (1.907)[d]	1.862
D_0 (eV)	2.17 (2.41)[b]	1.90	0.54	0.53	0.20
ω_e (cm^{-1})	624 (624.6 ± 0.2)[a]	597(590 ±7 0)[c]	535	560 (512 ± 2)[d]	624
T_e (cm^{-1})	0.0	1393 (1440 ± 80)[c]	11344	11574	14399
T_{00} (cm^{-1})			11298	11533 (11335)[d]	14407
Osc. str.			5.5×10^{-5}	1.9×10^{-3}	
T_{10} (cm^{-1})			11811	12058 (11847)[d]	
Osc. str.			1.3×10^{-5}	0.9×10^{-3}	
T_{01} (cm^{-1})				10925 (10726)[d]	
Osc. str.				0.8×10^{-3}	
T_{12} (cm^{-1})				10853 (10665)[d]	
Osc. str.				0.9×10^{-3}	

$T_{v'v''}$ values are given for the $a\,^4\Sigma^- - X\,^2\Pi_{3/2}$ transition. [a] Reference 2. [b] Assuming a Morse oscillator, ref 2. [c] Photoelectron spectroscopy of AuO$^-$, ref 3. [d] This work.
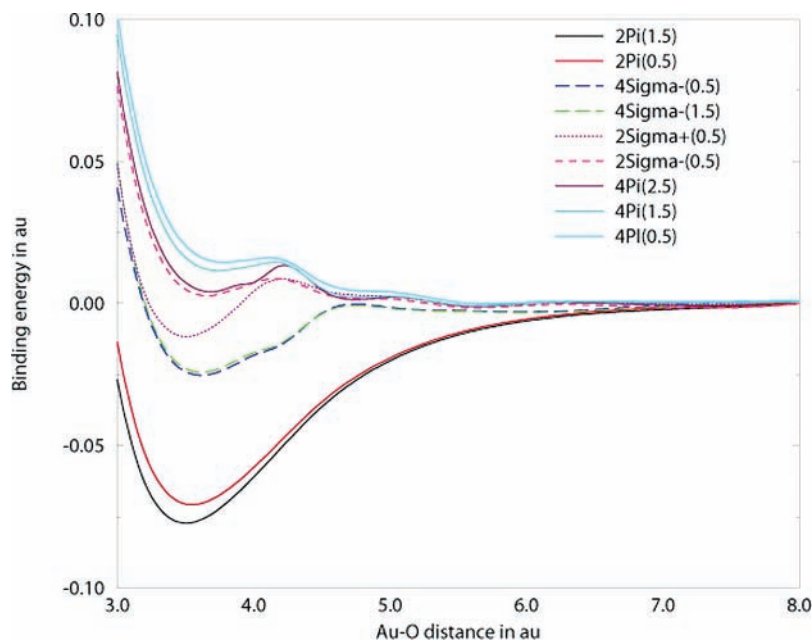
Figure 1. The potential curves for AuO that dissociate to Au(d^{10}s,^{2}S) plus O(p^4,^{3}P).

of this state, namely, the $a^4\Sigma^-_{3/2}$ level. The T_e value is 11574 cm^{-1}, with a vibrational frequency $\omega_e = 560$ cm^{-1}. The oscillator strength for the $a^4\Sigma^-_{3/2} - X^2\Pi_{3/2}$ transition is significantly larger than for the $a^4\Sigma^-_{1/2} - X^2\Pi_{3/2}$ transition (cf. Table 1). On the basis of the term energies for the two $^4\Sigma^-$ components,[10] the spin−spin parameter for the $a^4\Sigma^-$ state is estimated to be $\lambda = 57.5$ cm^{-1} where the splitting is given by $4\lambda = E(^4\Sigma^-_{3/2}) - E(^4\Sigma^-_{1/2})$. As will be discussed later, based on the bond length, term energy, calculated oscillator strength, and observed branches for the transition, we have assigned the upper state in the near-infrared electronic spectrum to the $a^4\Sigma^-_{3/2}$ state.

The next state is the A $^2\Sigma^+_{1/2}$ state with a T_e value of 14399 cm^{-1}, well separated from the lower states. For states with higher excitation energies we have only computed the vertical excitation levels, and these are presented in Table 2. To our knowledge they have not be studied experimentally. Calculated permanent electric dipole moments for the lowest five levels of AuO are given in Table 2.

Experimental Procedure

The method used to produce the AuO radicals and record the spectrum are reported previously.[1] Briefly, the gas-phase AuO molecules were produced in a neon-based electronic

TABLE 2: Calculated Vertical Excitation Energies (T_v) and Dipole Moments (μ) for the Lowest States of AuO

state	energy (cm^{-1})	dipole moment (Debye)
$^2\Pi_{3/2}$	0	4.44
$^2\Pi_{1/2}$	1430	4.44
$^4\Sigma^-_{3/2}$	11689	0.40
$^4\Sigma^-_{1/2}$	11993	0.40
$^2\Sigma^+_{1/2}$	14401	5.46
$^2\Sigma^-_{1/2}$	18125	0.39
$^4\Pi_{5/2}$	18563	
$^4\Pi_{3/2}$	20531	
$^4\Pi_{1/2}$	21438	

discharge using a gold-lined hollow cathode with a trace amount of oxygen. The Fourier transform spectrometer associated with the McMath−Pierce Solar telescope was configured with CaF$_2$ beam splitter and liquid-nitrogen-cooled InSb detector, to record the 4000−12000-cm^{-1} region.

Results and Discussion

From discrepancies in the ground-state rotational constants between the near-infrared analysis[1] and the microwave analysis,[2] it was clear that the rotational assignments of the near-infrared spectrum were incorrect. By use of the microwave constants[1] to calculate the energy levels of the $X^2\Pi_{3/2}$ state and the method

TABLE 3: Molecular Parameters for AuO (in cm^{-1})

	T_v	B_v	D_v x 10^6	q_{Jv} x 10^5
$X^2\Pi_{3/2}$ $v = 0$	0.0	0.331860359	0.38109	0.0
$X^2\Pi_{3/2}$ $v = 1$	614.566^{a,b}	0.328788044^{a,b}	0.38332^{a,b}	0.0^{a,b}
$X^2\Pi_{3/2}$ $v = 2$	1189.034^{a,b}	0.325735(10)	0.3868(19)	0.0^a
$A^4\Sigma^-_{3/2}$ $v = 0$	11335.0846(8)	0.31161425(73)	0.39492(13)	−0.46913(34)
$A^4\Sigma^-_{3/2}$ $v = 1$	11847.8875(8)	0.308143(10)	0.4074(18)	−0.46722(44)

^{a} Held fixed in fit. ^{b} From ref 2.

of combination differences, it became clear that the 10726-cm^{-1} band involved emission to the $v = 1$ ground electronic state. The 10665-cm^{-1} band did not connect with either the $v = 0$ or 1 levels of the ground electronic state.

In the infrared spectrum, four branches were identified in each band, two P-branches and two R-branches. With a spacing between the two bandheads of 61 cm^{-1}, these transitions are clearly not a vibrational progression but rather a vibrational sequence. A vibrational sequence is also consistent with the observed relative intensity of the two bands, where the 10726-cm^{-1} band is approximately 50% more intense than the 10665-cm^{-1} band. Previously assigned as the (0,0) and (1,1) bands of a $^2\Pi_{3/2} - {}^2\Pi_{3/2}$ transitions, we now believe they are the (0,1) and (1,2) bands of a $\Omega = 3/2 - X^2\Pi_{3/2}$ transition.

The new vibrational assignments prompted us to take another look at the spectrum in search of the (0,0) band for this transition, which should be located near 11340 cm^{-1}. No molecular signal was observed in this region of the spectrum. We believe this is due to the loss of sensitivity of the FT instrument in this region. Although we recorded and transformed the 4000−12000-cm^{-1} region, the FT spectrometer equipped with a CaF$_2$ beam splitter and InSb detector loses sensitivity at energies greater than 11000 cm^{-1}, and thus the (0,0) band is outside of the working range of the instrument in this configuration.

A standard Hund's case (c) $\Omega = 3/2$ polynomial expression was used to represent the energy levels for the excited and ground states

$$T = T_v + B_vJ(J + 1) - D_vJ^2(J + 1)^2 \pm 0.5q_vJ(J + 1)(J + 0.5) \quad (1)$$

The upper/lower sign is used to designate the e/f levels. For the 10726-cm^{-1} band that connects to the $v = 1$ ground electronic state, the B_1 and D_1 rotational constants from Okabayashi et al.[2] were held fixed in the fit, and their hyperfine parameters were not included.

In the original analysis of O'Brien et al.,[1] a λ doubling parameter was determined for each state, and the e/f symmetry was assigned so that the ground-state lambda-doubling parameter would be negative, consistent with the unique perturber model for the ground state.[11] However, in the microwave work, the data for $v = 0,1$ included line positions from $J = 6.5$ to $J = 19.5$, and q_J was not required in the fit.[2] When we refit the near-infrared lines, using the ground-state rotational constants from Okabayashi et al.[2] and $q_J = 0$, the fit was equally good, with improved precision on q_J of the excited state. Although this analysis thus gives more precise constants, it is now impossible to assign the e/f symmetry unambiguously. Clearly the assigned P$_e$ and R$_e$ branches connect to the same excited-state levels, and the assigned P$_f$ and R$_f$ branches connect to the other excited-state levels, but the absolute e/f assignments are arbitrary. The e/f symmetry assignments presented here remain unchanged from O'Brien et al.[1]

The ground state ω_e and $\omega_e x_e$ values were calculated by Okabayashi et al.[2] based on the Kratzer and Pekeris relationships.[11] These values were used to calculate the T_0, T_1, and T_2 levels for the $X^2\Pi_{3/2}$ state. For the experimental results reported here, T_0 was set to 0.0 cm^{-1}, and the zero point energy was subtracted from T_1 and T_2. The term energies based on $T_0 = 0.0$ cm^{-1} were used in our fits.

A total of 462 lines were included in the fit, with an average residual of the unblended lines of 0.004 cm^{-1}, which is consistent with the experimental uncertainty. Line positions, assignments, and fit residuals are presented in the Supporting Information. The molecular parameters determined by the fit are given in Table 3.

By use of B_0 and B_1 from Okabayashi et al.[1] and our B_2 value for the ground electronic state, the Dunham parameters can be determined for the equation $B_v = B_e - \alpha_e(v + {}^1/_2)$, $B_e = 0.333391233$ cm^{-1} (calculated 0.3287 cm^{-1}) and $\alpha_e = 0.003065477$ cm^{-1}. By use of the equilibrium rotational constant, the ground-state bond length can be determined, $r_e = 1.8488$ Å (calculated 1.861 Å).

By use of B_0 and B_1 for the excited state, the excited-state Dunham parameters can be determined, $B_e = 0.31334988$ cm^{-1} (calculated as 0.3113, see discussion below) and $\alpha_e = 0.00347125$ cm^{-1}. The excited-state bond length is determined to be $r_e = 1.9070$ Å.

On the basis of the electronic structure calculations, the excited $\Omega = 3/2$ state was identified as the $a^4\Sigma^-_{3/2}$ state. This assignment for the upper state is consistent with the calculated bond length, $r_{e,\text{expt}} = 1.9070$ Å and $r_{e,\text{calc}} = 1.924$ Å. The agreement between the calculated and observed transition energies is remarkable (see Table 1); only ∼200 cm^{-1} difference, which is less than 2% error of the transition energy. The assignment of the spectrum as a Hund's case (a) $^4\Sigma^-_{3/2} - X^2\Pi_{3/2}$ transition is also consistent with the observed branches in the spectrum, namely, two P-branches and two R-branches and no observed Q-branch. Although assignment of the upper state of our transition to the $a^4\Sigma^-_{1/2}$ state is possible, the spin−spin splitting in the $^4\Sigma^-_{1/2}$ state is expected to be very large and six observed branches would be expected.[10] Based on the change in dipole moment (see Table 2), the excitation to the $a^4\Sigma^-$ state is clearly a charge-transfer transition with charge moving to gold, as expected.

Conclusions

New theoretical work on AuO clarifies the electronic structure. Potential energy curves and spectroscopic parameters are calculated for the first five electronic states of AuO. The near-infrared electronic spectrum of AuO has been reanalyzed, and the 10726- and 10665-cm^{-1} bands are now assigned as the (0,1) and (1,2) bands of the $a^4\Sigma^-_{3/2} - X^2\Pi_{3/2}$ transition, respectively.

Electronic Spectrum of AuO

J. Phys. Chem. A, Vol. 110, No. 43, 2006 **11957**

Supporting Information Available: Line positions, assignments, and fit residuals for the (0,1) and (1,2) bands of the $a^4\Sigma^-_{3/2} - X^2\Pi_{3/2}$ transition are presented in Supporting Information. This material is available free of charge via the Internet at http://pubs.acs.org.

References and Notes

(1) O'Brien, L. C.; Hardimon, S. C.; O'Brien, J. J. *J. Phys. Chem. A* **2004**, *108*, 11302−11306.

(2) Okabayashi, T.; Koto, F.; Tsukamoto, K.; Yamazaki, E.; Tanimoto, M. *Chem. Phys. Lett.* **2005**, *403*, 223−227.

(3) Ichino, T.; Gianola, A. J.; Andrews, D. H.; Lineberger, W. C. *J. Phys. Chem. A* **2004**, *108*, 11307−11313.

(4) Roos, B. O. *Advanced Chemical Physics; Ab Initio Methods in Quantum Chemistry*; Lawley, K. P., Ed.; John Wiley & Sons Ltd., Chichester, England, 1987; Vol. II, Chapter 69, p 399.

(5) Andersson, K.; Malmqvist, P.-A.; Roos, B. O.; Sadlej, A. J.; Wolinski, K. *J. Phys. Chem.* **1990**, *94*, 5483−5488.

(6) Andersson, K.; Malmqvist. P.-Å.; Roos, B. O. *J. Chem. Phys.* **1992**, *96*, 1218−1226.

(7) Roos, B. O.; Lindh, R.; Malmqvist, P.-Å.; Veryazov, V.; Widmark. P.-O. *J. Phys. Chem. A* **2005**, *109*, 6575−6579.

(8) Roos, B. O.; Malmqvist, P.-Å. *Phys. Chem. Chem. Phys.* **2004**, *6*, 2919−2927.

(9) Karlström, G.; Lindh, R.; Malmqvist, P.-Å.; Roos, B. O.; Ryde, U.; Veryazov, V.; Widmark, P.-O.; Cossi, M.; Schimmelpfennig, B.; Neogrady, P.; Seijo, L. *Comput. Mater. Sci.* **2003**, *28*, 222.

(10) Femenias, J. L.; Cheval, G.; Merer, A. J.; Sassenberg, U. *J. Mol. Spectrosc.* **1987**, *124*, 348−368.

(11) Lefebvre-Brion, H.; Field, R. W. *Perturbations in the Spectra of Diatomic Molecules*; Academic Press, 1986.